Supporting Information

Practical Synthesis and Properties of 2,5-Diarylarsoles

Makoto Ishidoshiro, Yoshimasa Matsumura, Hiroaki Imoto, Yasuyuki Irie, Takuji Kato, Seiji Watase, Kimihiro Matsukawa, Shinsuke Inagi, Ikuyoshi Tomita, Kensuke Naka*

Contents:

1. Materials

Phenlyacetylene, titanium tetraisopropoxide ($Ti(O^iPr)_4$), sodium sulfate (Na_2SO_4), dichloromethane (CH_2Cl_2), dichlorophenylphosphine and methanol (MeOH) were purchased from Nacalai Tesque, Inc. Activated alumina, diethyl ether (Et_2O), iodine (I_2) and distilled water were purchased from Wako Pure Chemical Industry, Ltd. Isopropylmagnesium chloride (^{i}PrMgCl) and gold(I) chloride (AuCl) were purchased from Sigma-Aldrich Co. **1**[1] and *o*-methoxy-phenylacetylene[2] were prepared by following the literatures. Phenylacetylene, dichlorophenylphosphine and $Ti(O^iPr)_4$ were used after distillation under reduced pressure. Other commercially available chemicals were used without further purification. Tetrahydrofuran (THF) for cyclic voltammetry was dried over sodium benzophenone ketyl and distilled under nitrogen.

2. Measurements

^{1}H (400 MHz) and ^{13}C (100 MHz) NMR spectra of **5**, **6a** and **5**−AuCl were recorded on a Bruker DPX-400 spectrometers, and ^{1}H (300 MHz) and ^{13}C (75 MHz) NMR spectra of **6a**−AuCl were on a JEOL ECP-300 instrument. The samples were analyzed in $CDCl_3$ using Me_4Si as an internal standard. The following abbreviations are used; s: singlet, d: doublet, t: triplet, m: multiplet. High-resolution mass spectra (HRMS) were obtained on a JEOL JMS-SX102A spectrometer. The UV-vis spectra were recorded on a Jasco spectrophotometer V-670 KKN. Emission spectra were obtained on a JASCO fluorescence spectrophotometer FP-8500. Lifetimes of fluorescence were recorded in $CHCl_3$ at ambient temperature on a HORIBA Delta Flex. Cyclic voltammetric analyses were carried out on a Versa STAT3 (Princeton Applied Research) potentiostat at the scan rate of 100 $mV \cdot s^{-1}$. All the measurements were performed in distillated THF containing 0.1 M tetrabutylammonium hexafluorophosphate at ambient temperature using a three-electrode system, with each solution being purged with N_2 prior to measurement. The working electrode was a platinum (Pt) disk (d = 1.6 mm, BAS, Japan), the counter electrode was a Pt plate (1 x 1 cm^2), and the reference electrode was a silver (Ag) wire.

3. X-ray crystallographic data for single crystalline products

The single crystal was mounted on glass fibers with epoxy resin. Intensity data were collected at room temperature on a Rigaku RAXIS RAPID II imaging plate area detector with graphite monochromated Mo Kα radiation. The crystal-to-detector distance was 127.40 mm. Readout was performed in the 0.100 mm pixel mode. The data were collected at room temperature to a maximum 2θ value of 55.0°. Data were processed by the PROCESS-AUTO[3] program package. An empirical or numerical

absorption correction[4] was applied. The data were corrected for Lorentz and polarization effects. A correction for secondary extinction[5] was applied. The structure was solved by heavy atom Patterson methods[6] and expanded using Fourier techniques.[7] Some non-hydrogen atoms were refined anisotropically, while the rest were refined isotropically. Hydrogen atoms were refined using the riding model. The final cycle of full-matrix least-squares refinement on F^2 was based on observed reflections and variable parameters. In the case of the crystalline product recrystallized from acetone, the final cycle of full-matrix least-squares refinement on F was based on observed reflections and variable parameters. All calculations were performed using the CrystalStructure[8,9] crystallographic software package except for refinement, which was performed using SHELXL97.[10] Crystal data and more information on X-ray data collection are summarized in Table S1-S7.

4. Syntheses

*1,2,5-Triphenylarsole (**5a**)*

An Et_2O solution (10 mL) of phenylacetylene (0.22 mL, 2.0 mmol) and $Ti(O^iPr)_4$ (0.42 mL, 1.4 mmol) was cooled to -78 °C under argon atmosphere. To the solution was added an Et_2O solution of ^{i}PrMgCl (2.0 M, 1.4 mL, 2.8 mmol). The reaction mixture was stirred at -78 °C for 1 h, and at -50 °C for 4 h to obtain solution A. An Et_2O solution of I_2 (0.310 g, 1.22 mmol) was separately prepared, and **1** (0.195 g, 0.21 mmol) was dissolved in the solution under argon atmosphere to obtain solution B. To solution A was added solution B, and the reaction mixture was stirred at -50 °C for 2 h. The reaction mixture was poured into distilled water, and the products were extracted by CH_2Cl_2. The combined organic layer were dried over Na_2SO_4. After filtration, the solvents were removed in vacuo. The residue was subjected to column chromatography on activated alumina (eluent: hexane) to obtain **5a** (0.248 g, 0.696 mmol, 70%). ^{1}H NMR ($CDCl_3$, 400 MHz) δ 7.50 (d, J = 7.2 Hz, 4H), 7.43 (d, J = 4.8 Hz, 2H), 7.28-7.24 (m, 4H) 7.20-7.18 (m, 5H) ppm. ^{13}C NMR ($CDCl_3$, 100 MHz) δ 156.9, 137.6, 135.8, 133.8, 132.9, 128.9, 128.8, 128.7, 127.4, 126.4 ppm. HRMS (FAB) calcd. for $C_{22}H_{17}As$ $[M]^+$: 356.0546, found 356.0548.

*2,5-Bis(o-methoxyphenyl)-1-phenyl-arsole (**5b**)*

An Et_2O solution (10 mL) of *o*-methoxy phenylacetylene (0.264 g, 2.0 mmol) and $Ti(O^iPr)_4$ (0.42 mL, 1.4 mmol) was cooled to -78 °C under argon atmosphere. To the solution was added an Et_2O solution of ^{i}PrMgCl (2.0 M, 1.4 mL, 2.8 mmol). The reaction mixture was stirred at -78 °C for 1 h, and at -50 °C for 4 h to obtain solution A.

An Et_2O solution of I_2 (0.310 g, 1.22 mmol) was separately prepared, and **1** (0.195 g, 0.21 mmol) was dissolved in the solution under argon atmosphere to obtain solution B. To solution A was added solution B, and the reaction mixture was stirred at -50 °C for 2 h. The reaction mixture was poured into distilled water, the products were extracted by CH_2Cl_2. The combined organic layer were dried over Na_2SO_4. After filtration, the solvents were removed in vacuo. The residue was subjected to column chromatography on activated alumina (eluent: hexane) to obtain **5b** (0.316 g, 0.759 mmol, 76%). ^{1}H NMR ($CDCl_3$, 400 MHz) δ 7.62 (s, 2H), 7.58 (d, J = 6.0 Hz, 2H), 7.37-7.35 (m, 2H), 7.14-7.10 (m, 5H), 6.90-6.81 (m, 4H), 3.72 (s, 6H) ppm. ^{13}C NMR ($CDCl_3$, 100 MHz) δ 156.2, 152.7, 138.2, 135.0, 132.6, 128.3, 127.9, 127.8, 127.7, 127.0, 120.7, 111.4, 55.0 ppm. HRMS (FAB) calcd. for $C_{24}H_{21}O_2As$ $[M]^+$: 416.0758, found 416.0768.

*1,2,5-Triphenylphosphole (**6a**)*

An Et_2O solution (10 mL) of phenylacetylene (0.22 mL, 2.0 mmol) and $Ti(O^iPr)_4$ (0.42 mL, 1.4 mmol) was cooled to -78 °C under argon atmosphere. To the solution was added an Et_2O solution of ^{i}PrMgCl (2.0 M, 1.4 mL, 2.8 mmol). The reaction mixture was stirred at -78 °C for 1 h, and at -50 °C for 4 h. To the solution was added dichlorophenylphosphine (0.16 mL, 1.2 mmol), and the reaction mixture was stirred at -50 °C for 2 h. The reaction mixture was poured into distilled water, the products were extracted by CH_2Cl_2. The combined organic layer were dried over Na_2SO_4. After filtration, the solvents were removed in vacuo. The residue was subjected to column chromatography on activated alumina (eluent: hexane) to obtain **6a** (0.202 g, 0.645 mmol, 65%). ^{1}H NMR ($CDCl_3$, 400 MHz) δ 7.54 (d, J = 8.4 Hz, 4H), 7.39 (t, J = 8.0 Hz, 2H), 7.30-7.25 (m, 6H), 7.19-7.15 (m, 5H) ppm. ^{13}C NMR ($CDCl_3$, 100 MHz) δ 151.5, 136.3 (J = 16.6 Hz), 133.8 (J = 19.1 Hz), 132.0 (J = 9.0 Hz), 130.8 (J = 8.2 Hz), 129.6, 128.8 (J = 8.6 Hz), 128.6, 127.2, 126.4 ppm. HRMS (FAB) calcd. for. $C_{22}H_{17}P$ $[M]^+$: 312.1068, found 312.1071.

*Au(I)Cl complex with **5a** (**5a**−AuCl)*

A CH_2Cl_2 solution (1 mL) of 1 (20.2 mg, 0.0567 mmol) and AuCl (13.5 mg, 0.0582 mmol) was stirred at room temperature under nitrogen atmosphere. After stirring for 3 h, the solvents were removed in vacuo. The obtained product was subjected to recrystallization from CH_2Cl_2 and MeOH to obtain **5a**−AuCl (26.0 mg, 0.0441 mmol, 78%) as yellow solid. ^{1}H NMR ($CDCl_3$, 400 MHz) δ 7.69 (d, J = 6.8 Hz, 2H), 7.57 (dd, J = 1.6, 7.8 Hz, 4H), 7.48-7.37 (m, 5H), 7.34-7.28 (m, 6H) ppm. ^{13}C NMR ($CDCl_3$, 100 MHz) δ 151.5, 136.3 (J = 16.6 Hz), 133.8 (J = 19.1 Hz), 132.0 (J = 9.0 Hz), 130.8 (J =

8.2 Hz), 129.6, 128.8 (J = 8.6 Hz), 128.6, 127.2, 126.4 (J = 9.5 Hz) ppm. HRMS (FAB) calcd. for $C_{22}H_{17}ClAsAu$ $[M]^+$: 587.9900, found 587.9908.

*Au(I)Cl complex with **5b** (**5b**−AuCl)*

A CH_2Cl_2 solution (1 mL) of **1** (18.9 mg, 0.0454 mmol) and AuCl (10.4 mg, 0.0448 mmol) was stirred at room temperature under nitrogen atmosphere. After stirring for 2 h, the solvents were removed in vacuo. The obtained product was subjected to recrystallization from CH_2Cl_2 and MeOH to obtain **5b**−AuCl (22.1 mg, 0.0325 mmol, 73%) as yellow solid. ^{1}H NMR ($CDCl_3$, 400 MHz) δ 7.67-7.65 (m, 3H), 7.64 (d, J = 1.6 Hz, 1H), 7.61-7.58 (m, 3H), 7.37-7.30 (m, 3H), 7.25-7.21 (m, 2H), 6.92 (t, J = 7.6 Hz, 2H), 6.82 (d, J = 8.4 Hz, 2H), 3.70 (s, 6H) ppm. ^{13}C NMR ($CDCl_3$, 100 MHz) δ 156.0, 141.4, 134.9, 131.7, 131.5, 130.5, 130.2, 129.1, 127.6, 122.9, 121.0, 111.4, 54.6 ppm. HRMS (FAB) calcd. for $C_{24}H_{21}O_2ClAsAu$ $[M]^+$: 648.0112, found 648.0114.

*Au(I)Cl complex with **6a** (**6a**−AuCl)*

To a dichloromethane (5 mL) solution of **6a** (0.031 g, 0.100 mmol), was added a dichloromethane (1.0 mL) solution of gold chloride tetrahydrothiophene complex (0.038 g, 0.120 mmol) at ambient temperature under argon and the mixture was stirred for 1 h. Then, the product was purified by recrystallization from dichloromethane and hexane to give **6a**−AuCl in 90% yield (0.049 g, 0.090 mmol) as yellow needle crystals. ^{1}H NMR (300 MHz, $CDCl_3$): 7.26-7.34 (6H), 7.36 (s, 1H), 7.37-7.39 (2H), 7.41-7.49 (2H), 7.61-7.66 (4H), 7.74 (dd, J = 1.7, 5.6 Hz, 2H); ^{13}C NMR (75 MHz, CDCl3): 127.0, 129.5, 130.2, 132.4, 132.6, 133.1, 134.8, 135.3, 142.3, 143.4. HRMS (FAB) calcd. for $C_{22}H_{17}AuClP$ $[M]^+$: 544.0422, found 544.0438.

5. NMR spectra

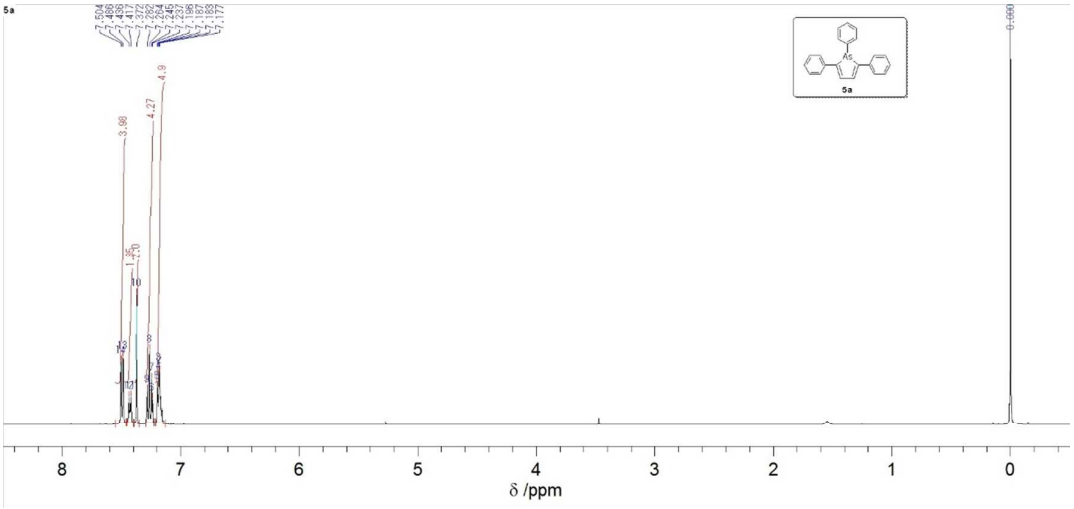

Figure S1. ^{1}H NMR spectrum (400 MHz) of **5a** in $CDCl_3$.

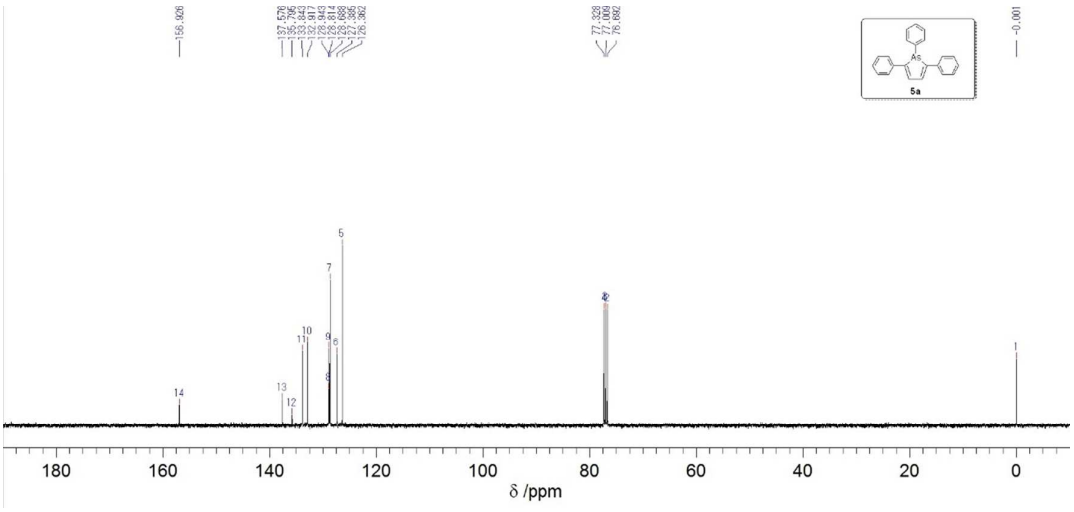

Figure S2. ^{13}C NMR spectrum (100 MHz) of **5a** in $CDCl_3$.

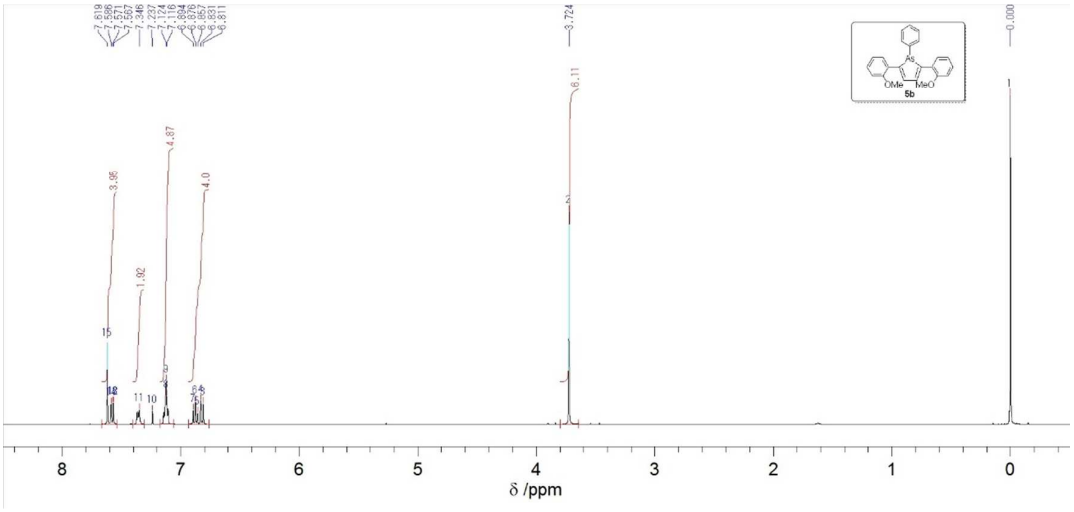

Figure S3. ^{1}H NMR spectrum (400 MHz) of **5b** in $CDCl_3$.

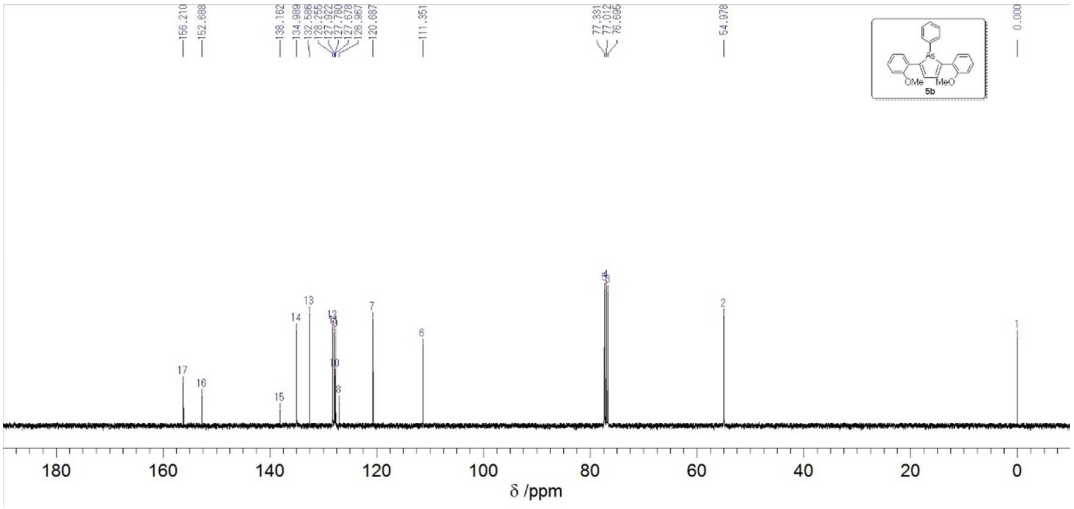

Figure S4. ^{13}C NMR spectrum (100 MHz) of **5b** in $CDCl_3$.

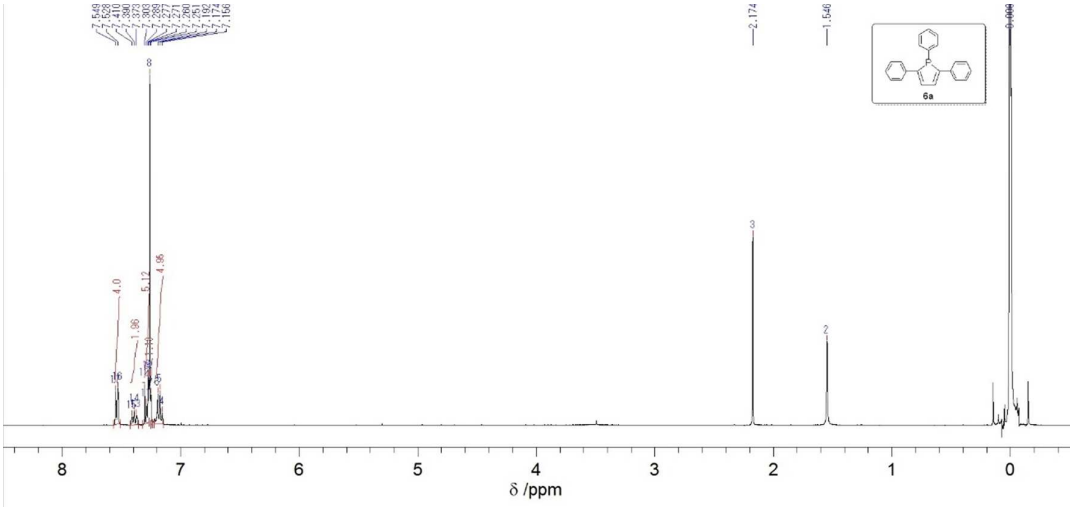

Figure S5. ^{1}H NMR spectrum (400 MHz) of **6a** in $CDCl_3$.

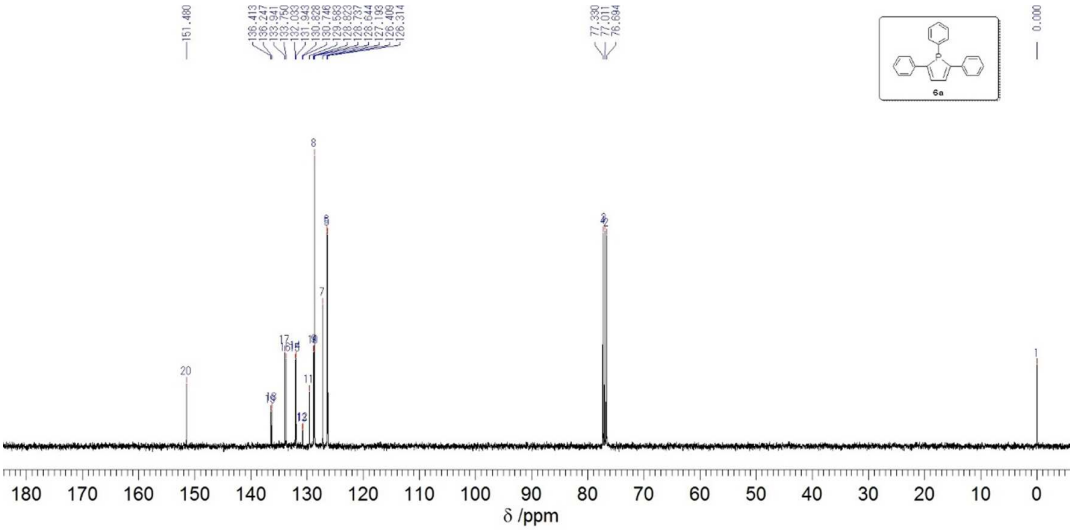

Figure S6. ^{13}C NMR spectrum (100 MHz) of **6a** in $CDCl_3$.

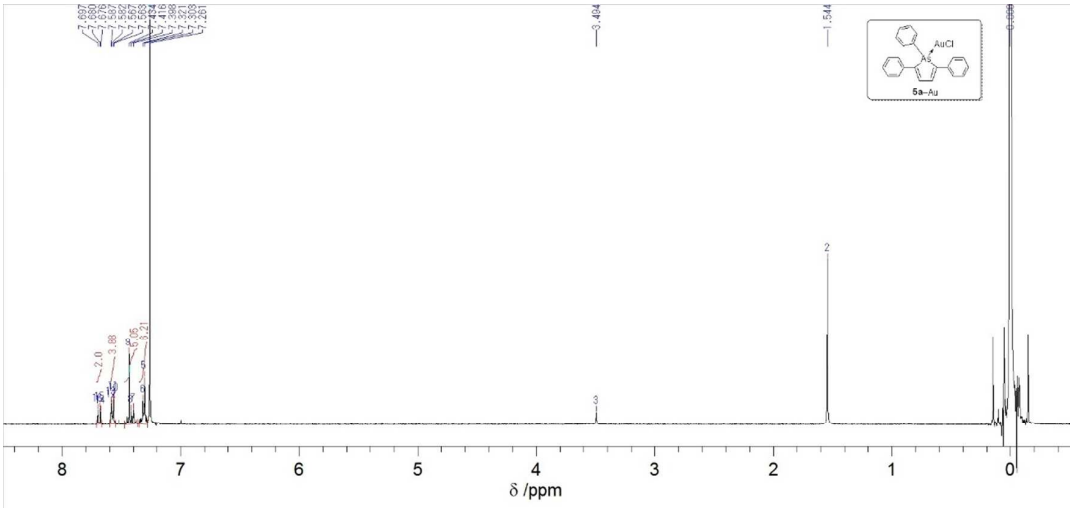

Figure S7. ^{1}H NMR spectrum (400 MHz) of **5a**−AuCl in $CDCl_3$.

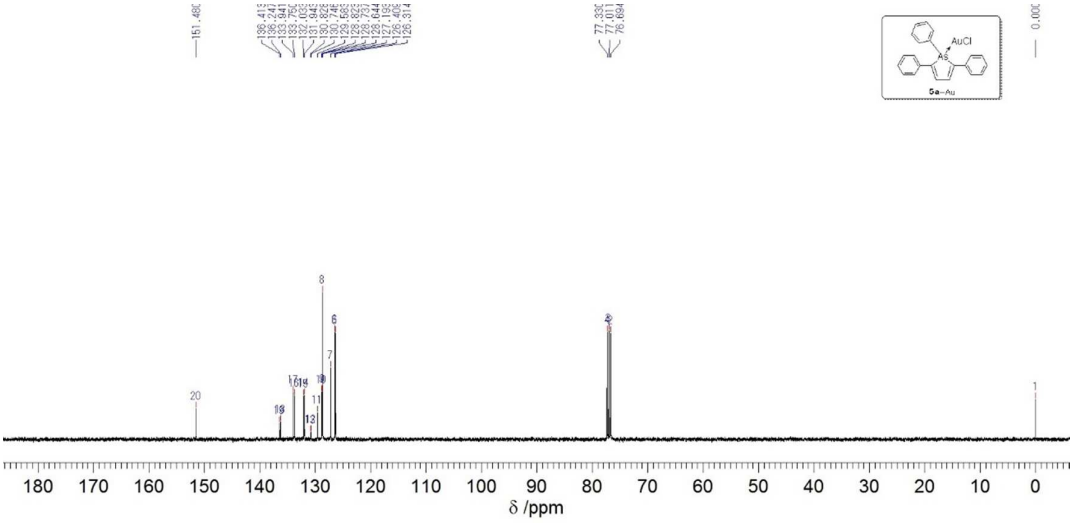

Figure S8. ^{13}C NMR spectrum (100 MHz) of **5a**−AuCl in $CDCl_3$.

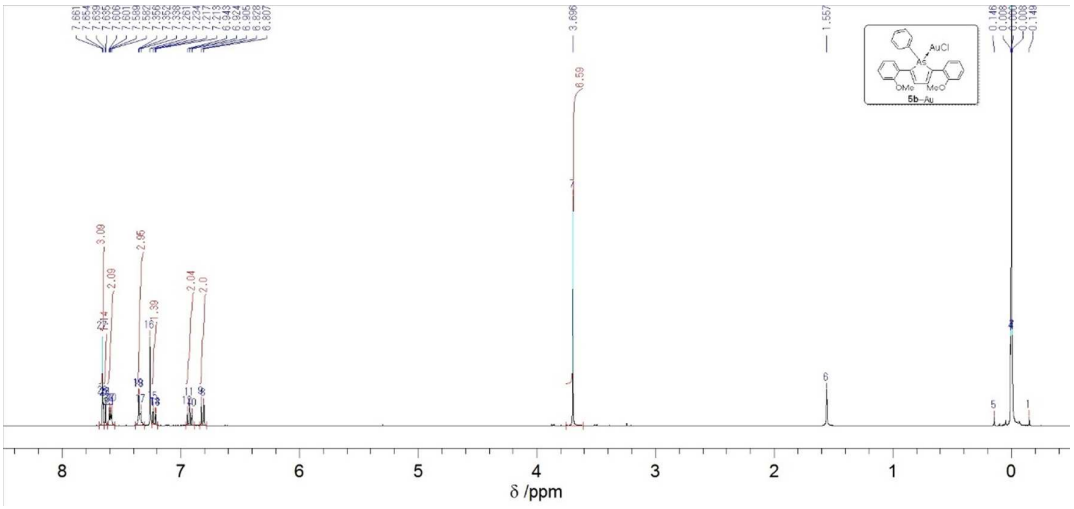

Figure S9. ^{1}H NMR spectrum (400 MHz) of **5b**−AuCl in $CDCl_3$.

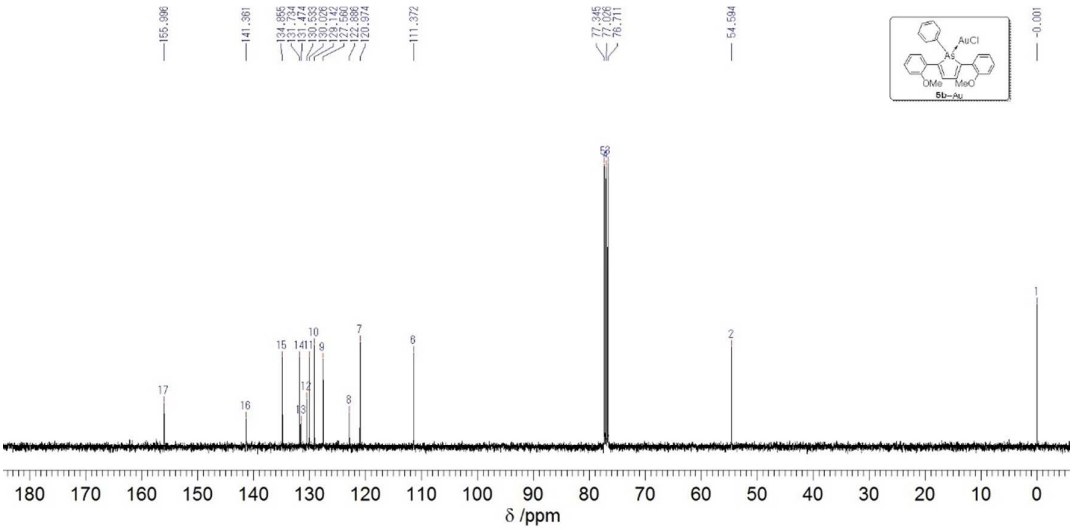

Figure S10. ^{13}C NMR spectrum (100 MHz) of **5b**−AuCl in $CDCl_3$.

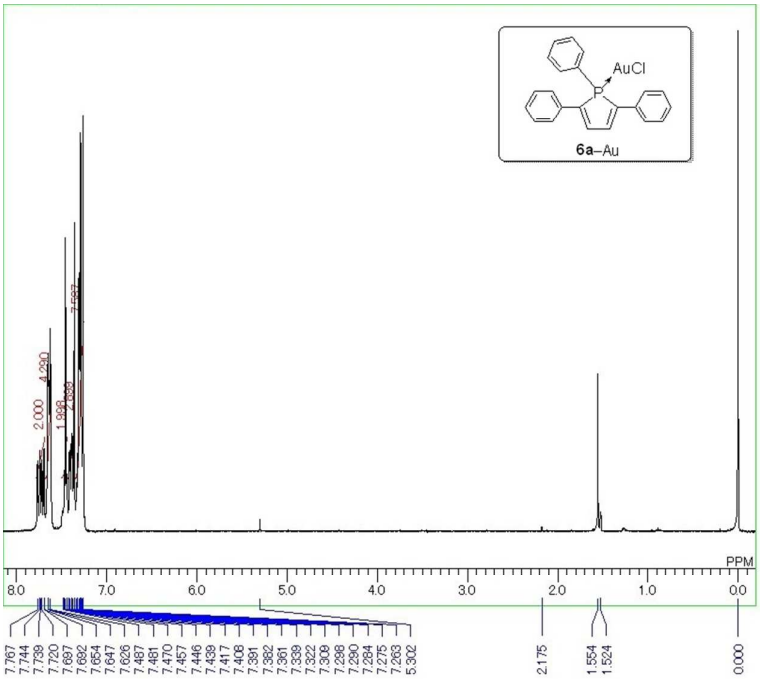

Figure S11. ^{1}H NMR spectrum (300 MHz) of **6a**−AuCl in $CDCl_3$.

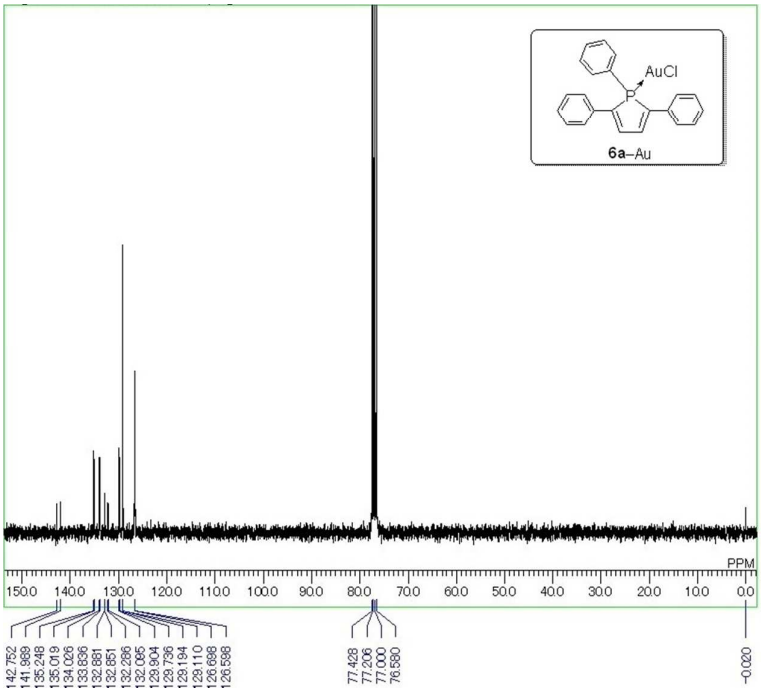

Figure S12. ^{13}C NMR spectrum (75 MHz) of **6a**−AuCl in $CDCl_3$.

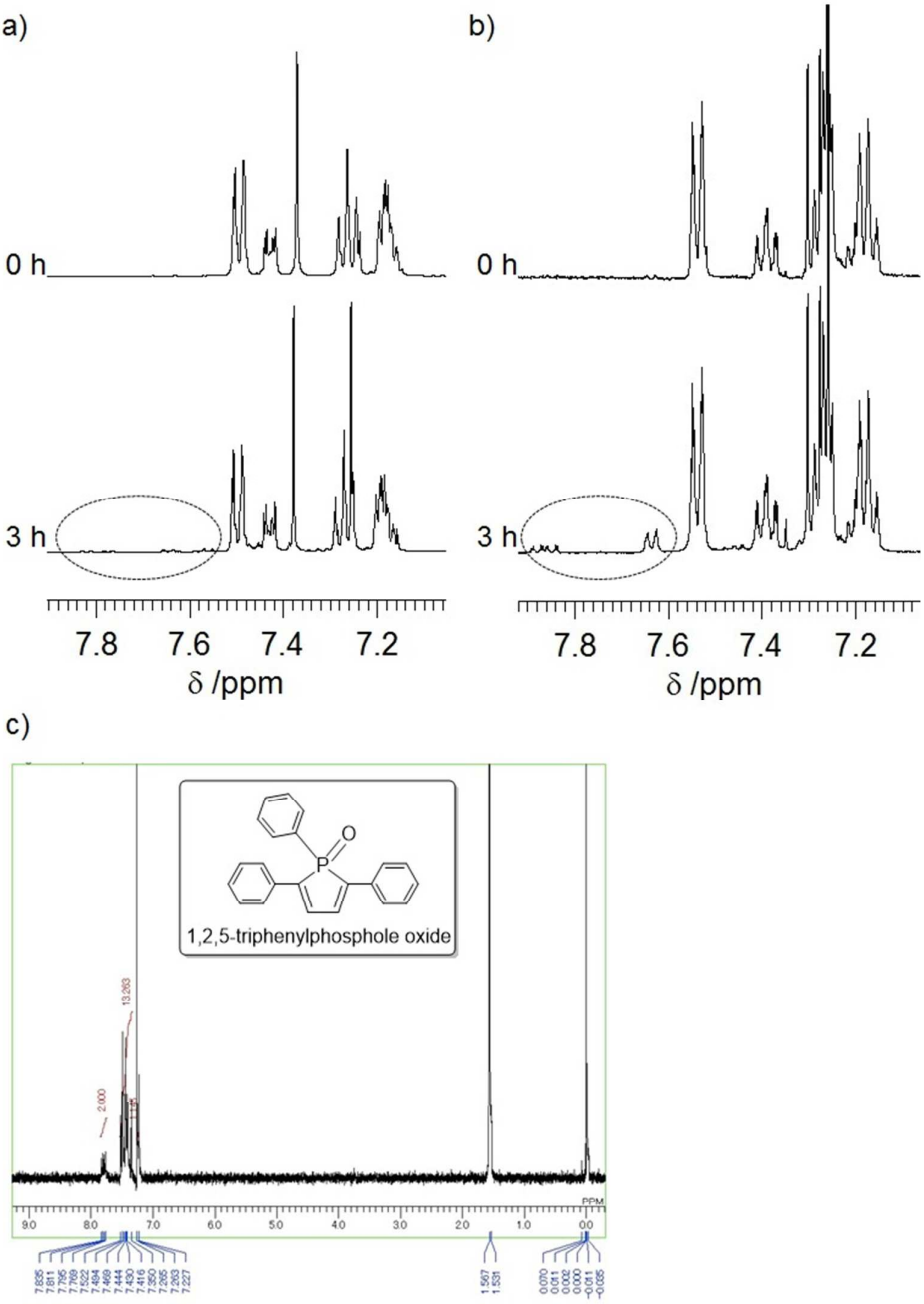

Figure S13. ^{1}H NMR spectra of a) **5a** and b) **6a** before and after the dry air-bubbling for 3 h. Dashed circles indicate the oxide signals. c) ^{1}H NMR spectrum of 1,2,5-triphenyl phosphole oxide, which was prepared according to the literature.[11] Although signals of oxidation of **5a** were too small to be defined and should be complicating,[12] very few amounts of **5a** (< 2%) was oxidized by air-bubbling.

6. Crystallographic data

Table S1. Crystallographic Data.

	5a	**5b**	**6a**
A. Crystal data			
Empirical Formula	C22H17As	C24H21AsO2	C22H17P
Formula Weight	356.30	416.35	312.35
Crystal Dimension, mm^3	0.200 × 0.200 × 0.100	0.400 × 0.250 × 0.200	0.200 × 0.180 × 0.100
Crystal System	monoclinic	orthorhombic	monoclinic
Space Group	$P2_1$	Pnma	$P2_1$
a, Å	12.2262(4)	7.88163(18)	12.1722(5)
b, Å	6.03311(18)	16.2823(4)	5.9237(2)
c, Å	12.5465(5)	15.3253(3)	12.6791(6)
α, deg	-	90.000	-
β, deg	115.2163(10)	90.000	115.8923(15)
γ, deg	-	90.000	-
Volume, $Å^3$	837.27(5)	1966.72(8)	822.44(6)
D_{calcd}, g cm^{-3}	1.413	1.406	1.261
Z	2	4	2
F(000)	364.00	856.00	328.00
Data Collection			
Temperature, deg	23.0	23.0	23.0
2θmax, deg	54.9	54.9	54.9
Tmin/Tmax	0.588 / 0.817	0.530 / 0.705	0.833 / 0.984
Refinement			
No. of Observed Data	3060	1980	2380
No. of Parameters	226	151	226
R1[a], wR2[b]	0.0246, 0.0409	0.0306, 0.0934	0.0308, 0.0618
Goodness of Fit Indictor	1.205	1.009	1.036

[a] $R1 = \Sigma \, | |Fo| - |Fc| | \, / \, \Sigma \, |Fo|$ [b] $wR2 = [\, \Sigma \, w \, ((Fo^2-Fc^2)^2 \, / \, \Sigma \, w \, (Fo^2)^2 \,]^{1/2}$ $w = [\, \sigma^2(Fo^2) \,]^{-1}$

CCDC #1418475 (**5a**), 1418477 (**5b**) and 1418478 (**5c**)

Table S2. Crystallographic Data for **5a**–AuCl and **6a**–AuCl.

	5a–AuCl	**6a**–AuCl
A. Crystal data		
Empirical Formula	C22H17AsAuCl	C22H17AuClP
Formula Weight	588.72	416.35
Crystal Dimension, mm^3	0.300 × 0.150 × 0.100	0.400 × 0.300 × 0.050
Crystal System	monoclinic	orthorhombic
Space Group	$P2_1$	Pbca
a, Å	8.5323(3)	9.915(3)
b, Å	19.1547(4)	17.298(5)
c, Å	12.0545(4)	22.652(6)
α, deg	-	90.000
β, deg	99.9913(11)	90.000
γ, deg	-	90.000
Volume, $Å^3$	1940.23(9)	3885.0(19)
D_{calcd}, g cm^{-3}	2.015	1.863
Z	4	8
F(000)	1112.00	2080.00
Data Collection		
Temperature, deg	23.0	23.0
2θmax, deg	54.9	54.9
Tmin/Tmax	0.258 / 0.389	-
Refinement		
No. of Observed Data	3287	4435
No. of Parameters	244	226
R1[a], wR2[b]	0.0271, 0.0534	0.0413, 0.0949
Goodness of Fit Indictor	1.045	0.934

[a] $R1 = \Sigma \mid |Fo| - |Fc| \mid / \Sigma |Fo|$

[b] $wR2 = [\ \Sigma\ w\ ((Fo^2-Fc^2)^2 / \Sigma\ w\ (Fo^2)^2\ ]^{1/2} \quad w = [\ \sigma^2(Fo^2)\ ]^{-1}$

CCDC #1418476 (**5a**–AuCl) and 1418479 (6**a**–AuCl)

Table S3. Selected angles (deg) and distance (Å) of **5a**.

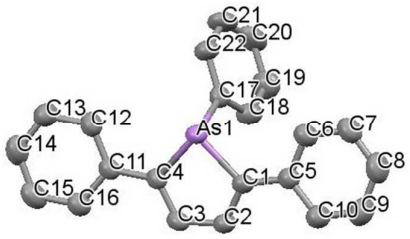

interplanar angles (°)	As(1)C(1)C(2)C(3)C(4)-C(5)C(6)C(7)C(8)C(9)C(10)	7.16
	As(1)C(1)C(2)C(3)C(4)-C(11)C(12)C(13)C(14)C(15)C(16)	9.44
distances (Å)	As(1)-C(1)	1.943(2)
	As(1)-C(4)	1.953(2)
	As(1)-C(17)	1.958(2)
	C(1)-C(2)	1.337(4)
	C(2)-C(3)	1.448(3)
	C(3)-C(4)	1.349(3)
	C(1)-C(5)	1.464(3)
	C(4)-C(11)	1.458(3)
angles (°)	C(1)-As(1)-C(4)	87.0(1)
	C(1)-As(1)-C(17)	101.8(1)
	C(4)-As(1)-C(17)	101.7(1)
	As(1)-C(1)-C(2)	109.2(2)
	C(1)-C(2)-C(3)	117.5(2)
	C(2)-C(3)-C(4)	117.2(2)
	As(1)-C(4)-C(3)	108.6(2)
	As(1)-C(1)-C(5)	124.0(2)
	As(1)-C(4)-C(11)	124.3(2)
	C(2)-C(1)-C(5)	126.5(2)
	C(3)-C(4)-C(11)	126.4(2)

Table S4. Selected angles (deg) and distances (Å) of **5b**.

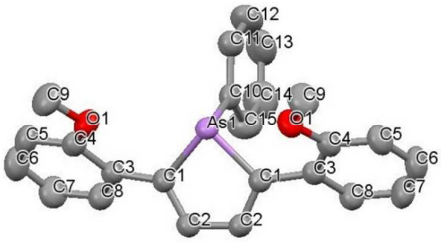

interplanar angles (°)	As(1)C(1)C(2)C(2)C(1)-C(3)C(4)C(5)C(6)C(7)C(8)	43.48
distances (Å)	As(1)-C(1)	1.960(2)
	As(1)-C(10)	1.969(3)
	C(1)-C(2)	1.343(3)
	C(2)-C(2)	1.449(3)
	C(1)-C(3)	1.474(3)
angles (°)	C(1)-As(1)-C(1)	86.28(7)
	C(1)-As(1)-C(10)	97.3(1)
	As(1)-C(1)-C(2)	109.4(1)
	C(1)-C(2)-C(3)	117.3(2)
	As(1)-C(1)-C(3)	126.5(1)
	C(2)-C(1)-C(3)	124.1(2)

Table S5. Selected angles (deg) and distance (Å) of **6a**.

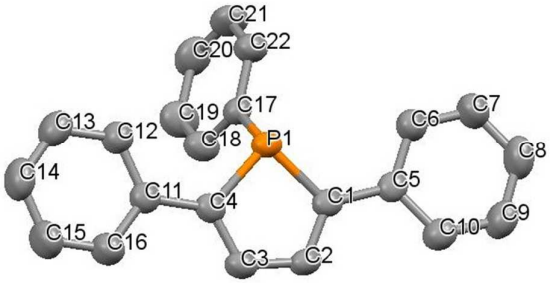

interplanar angles (°)	P(1)C(1)C(2)C(3)C(4)-C(5)C(6)C(7)C(8)C(9)C(10)	7.96
	P(1)C(1)C(2)C(3)C(4)-C(11)C(12)C(13)C(14)C(15)C(16)	4.52
distances (Å)	P(1)-C(1)	1.826(2)
	P(1)-C(4)	1.817(2)
	P(1)-C(17)	1.841(2)
	C(1)-C(2)	1.351(3)
	C(2)-C(3)	1.430(3)
	C(3)-C(4)	1.352(3)
	C(1)-C(5)	1.461(3)
	C(4)-C(11)	1.468(3)
angles (°)	C(1)-P(1)-C(4)	91.4(1)
	C(1)-P(1)-C(17)	105.6(1)
	C(4)-P(1)-C(17)	104.7(1)
	P(1)-C(1)-C(2)	107.8(2)
	C(1)-C(2)-C(3)	116.2(2)
	C(2)-C(3)-C(4)	115.4(2)
	P(1)-C(4)-C(3)	108.5(2)
	P(1)-C(1)-C(5)	124.9(2)
	P(1)-C(4)-C(11)	124.8(2)
	C(2)-C(1)-C(5)	126.3(2)
	C(3)-C(4)-C(11)	126.4(2)

Table S6. Selected angles (deg) and distance (Å) of **5a**−AuCl.

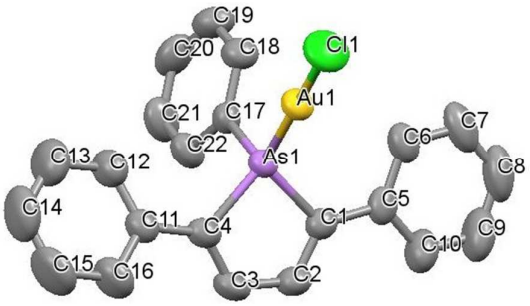

interplanar angles (°)	As(1)C(1)C(2)C(3)C(4)-C(5)C(6)C(7)C(8)C(9)C(10)	2.17
	As(1)C(1)C(2)C(3)C(4)-C(11)C(12)C(13)C(14)C(15)C(16)	23.54
distances (Å)	Au(1)-As(1)	2.3313(4)
	Au(1)Cl(1)	2.277(1)
	As(1)-C(1)	1.943(4)
	As(1)-C(4)	1.936(4)
	As(1)-C(17)	1.932(4)
	C(1)-C(2)	1.328(6)
	C(2)-C(3)	1.451(6)
	C(3)-C(4)	1.335(5)
	C(1)-C(5)	1.462(6)
	C(4)-C(11)	1.459(6)
angles (°)	Cl(1)-Au(1)-As(1)	175.54(4)
	Au(1)-As(1)-C(1)	119.7(1)
	Au(1)-As(1)-C(4)	117.0(1)
	Au(1)-As(1)-C(17)	117.9(1)
	C(1)-As(1)-C(4)	89.3(2)
	C(1)-As(1)-C(17)	103.6(2)
	C(4)-As(1)-C(17)	104.9(2)
	As(1)-C(1)-C(2)	106.8(3)
	C(1)-C(2)-C(3)	118.6(4)
	C(2)-C(3)-C(4)	118.6(4)
	As(1)-C(4)-C(3)	106.7(3)
	As(1)-C(1)-C(5)	123.9(3)
	As(1)-C(4)-C(11)	124.7(3)
	C(2)-C(1)-C(5)	129.3(4)
	C(3)-C(4)-C(11)	128.6(4)

Table S7. Selected angles (deg) and distance (Å) of **6a**−AuCl.

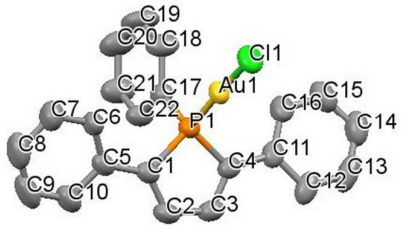

interplanar angles (°)	P(1)C(1)C(2)C(3)C(4)-C(5)C(6)C(7)C(8)C(9)C(10)	15.66
	P(1)C(1)C(2)C(3)C(4)-C(11)C(12)C(13)C(14)C(15)C(16)	15.72
distances (Å)	Au(1)-P(1)	2.225(2)
	Au(1)Cl(1)	2.279(2)
	P(1)-C(1)	1.807(5)
	P(1)-C(4)	1.811(5)
	P(1)-C(17)	1.796(5)
	C(1)-C(2)	1.348(8)
	C(2)-C(3)	1.438(8)
	C(3)-C(4)	1.345(8)
	C(1)-C(5)	1.450(7)
	C(4)-C(11)	1.466(8)
angles (°)	Cl(1)-Au(1)-P(1)	176.71(6)
	Au(1)-P(1)-C(1)	113.0(2)
	Au(1)-P(1)-C(4)	113.8(2)
	Au(1)-P(1)-C(17)	118.5(2)
	C(1)-P(1)-C(4)	93.9(2)
	C(1)-P(1)-C(17)	106.2(2)
	C(4)-P(1)-C(17)	108.4(2)
	P(1)-C(1)-C(2)	106.3(4)
	C(1)-C(2)-C(3)	116.8(5)
	C(2)-C(3)-C(4)	116.4(5)
	P(1)-C(4)-C(3)	106.4(4)
	P(1)-C(1)-C(5)	124.9(4)
	P(1)-C(4)-C(11)	124.5(4)
	C(2)-C(1)-C(5)	128.8(5)
	C(3)-C(4)-C(11)	129.0(5)

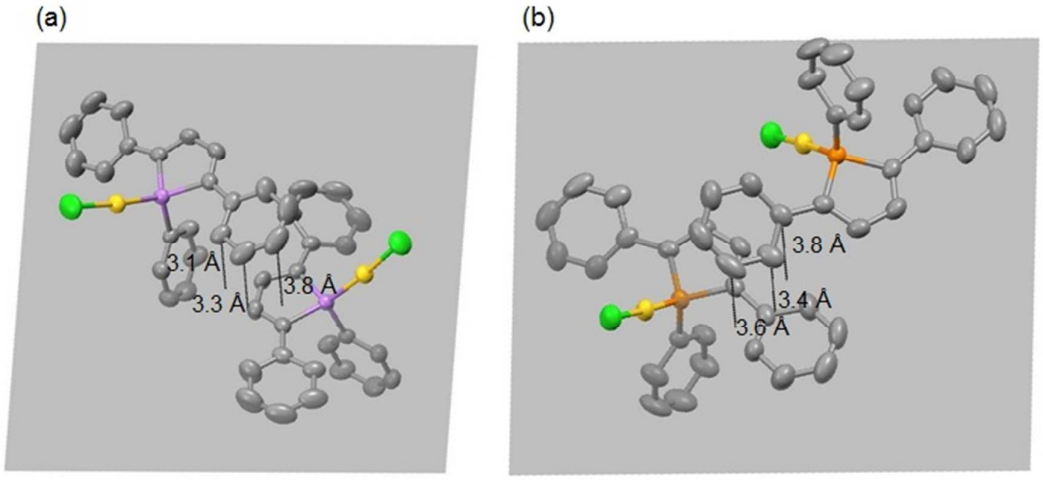

Figure S14. Packing structures of (a) **5a**–AuCl and (b) **6a**–AuCl for drawing π-π interactions.

7. Optical properties

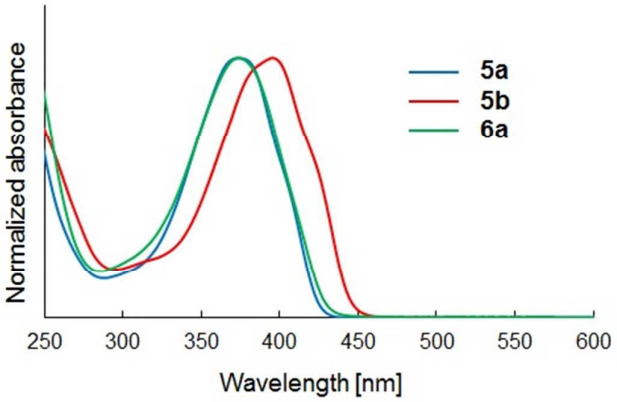

Figure S15. UV-vis absorption spectra of **5a**, **5b** and **6a** (in $CHCl_3$). The molar extinction coefficients at λ_{max} of **5a**, **5b** and **6a** were 3.5 x 10^4 $L \cdot mol^{-1} \cdot cm^{-1}$, 2.8 x 10^4 $L \cdot mol^{-1} \cdot cm^{-1}$ and 2.1 x 10^4 $L \cdot mol^{-1} \cdot cm^{-1}$, respectively.

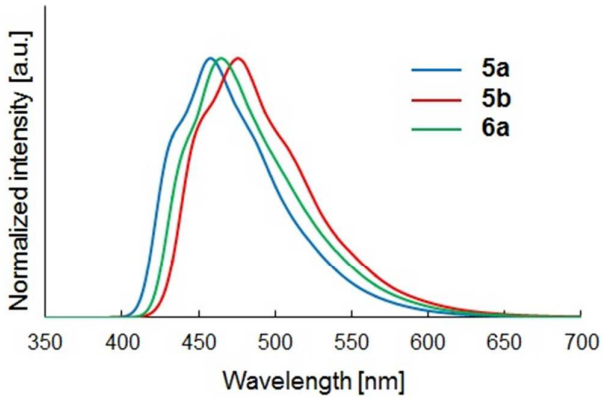

Figure S16. PL spectra of **5a**, **5b** and **6a** (in $CHCl_3$).

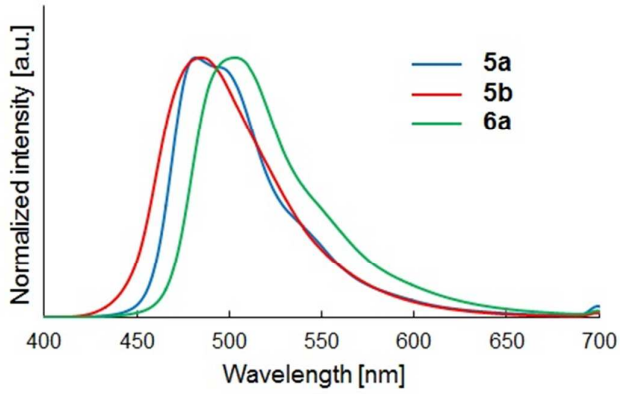

Figure S17. PL spectra of **5a**, **5b** and **6a** (in the solid states).

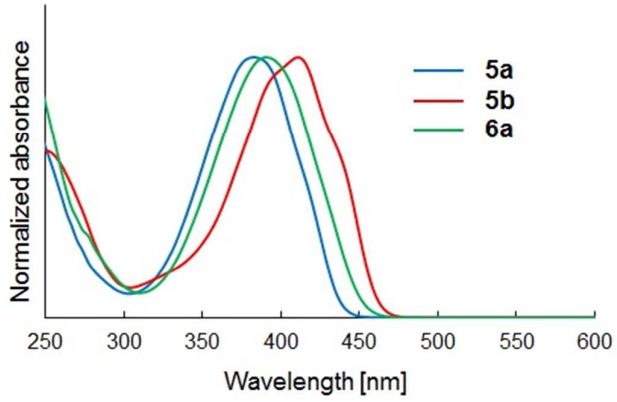

Figure S18. UV-vis absorption spectra of **5a**−AuCl, **5b**−AuCl and **6a**−AuCl (in $CHCl_3$). The molar extinction coefficients at λ_{max} of **5a**−AuCl, **5b**−AuCl and **6a**−AuCl were 1.9 x 10^4 L·mol^{-1}·cm^{-1}, 1.8 x 10^4 L·mol^{-1}·cm^{-1} and 1.8 x 10^4 L·mol^{-1}·cm^{-1}, respectively.

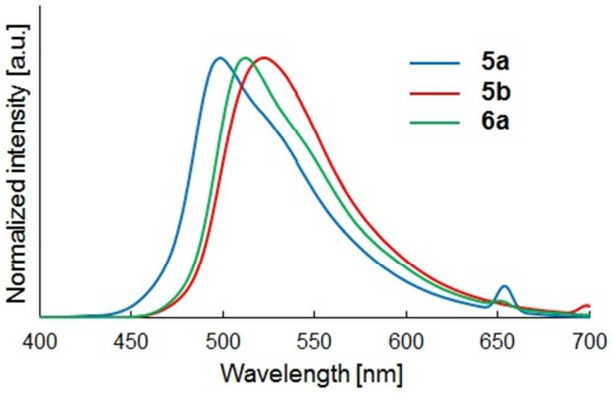

Figure S19. PL spectra of **5a**−AuCl, **5b**−AuCl and **6a**−AuCl (in the solid states).

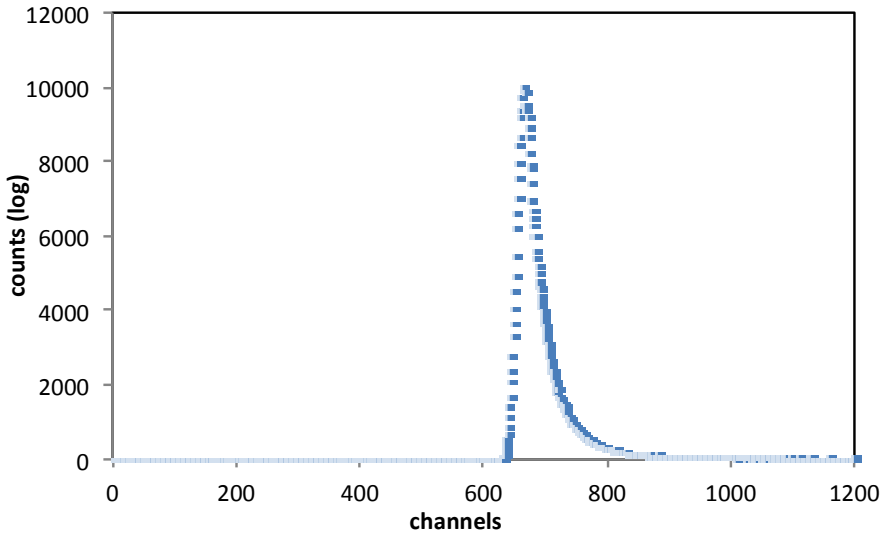

Figure S20. Decay plots of **5a** (measured in $CHCl_3$ at 25°C).

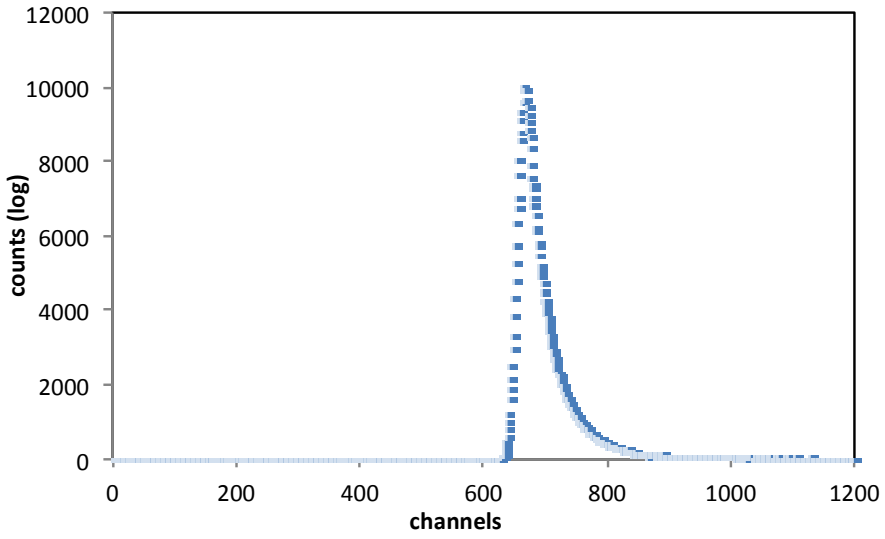

Figure S21. Decay plots of **5b** (measured in $CHCl_3$ at 25°C).

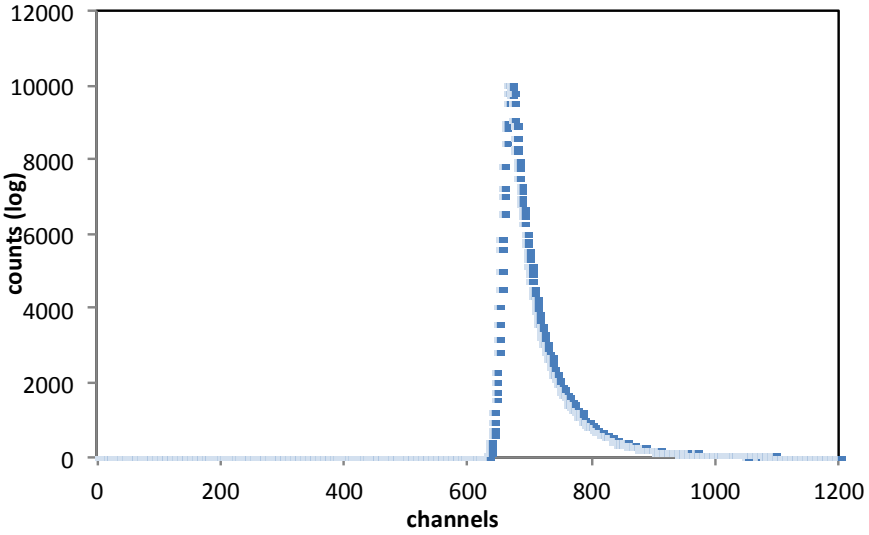

Figure S22. Decay plots of **6a** (measured in $CHCl_3$ at 25°C).

Table S8. Lifetime of fluorescence of **5a**, **5b** and **6a**.

product	$\tau_{1/2}$ [ns]
5a	2.92
5b	1.76
6a	2.06

8. Cyclic voltammetric analysis

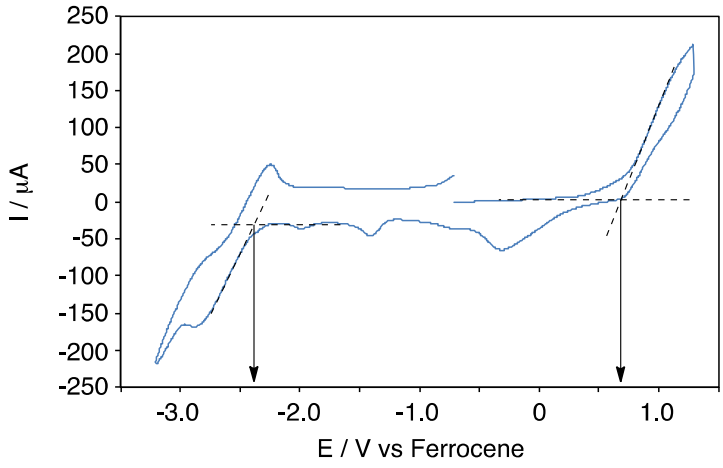

Figure S23. Cyclic voltammogram of **5a** in THF solution of tetra-*n*-butylammonium hexafluorophosphate (0.10 M), at a sweep rate of 100 $mV \cdot s^{-1}$.

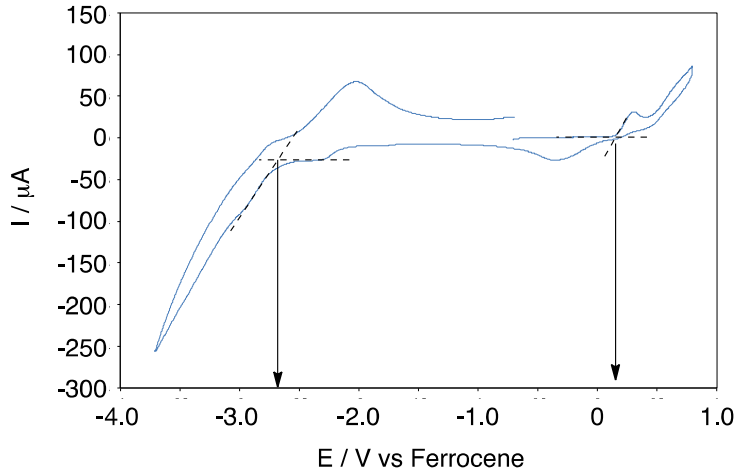

Figure S24. Cyclic voltammogram of **5b** in THF solution of tetra-*n*-butylammonium hexafluorophosphate (0.10 M), at a sweep rate of 100 $mV \cdot s^{-1}$.

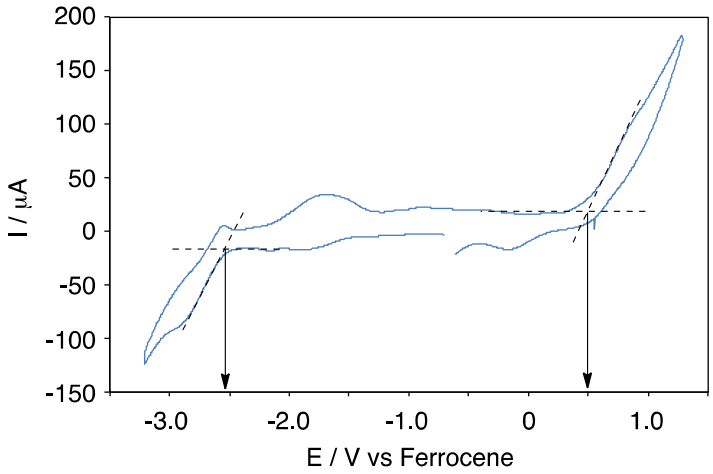

Figure S25. Cyclic voltammogram of **5b** in THF solution of tetra-*n*-butylammonium hexafluorophosphate (0.10 M), at a sweep rate of 100 $mV \cdot s^{-1}$.

Table S9. Electronic properties of **5a**, **5b** and **6a**.

product	E_{ox} [a] [V]	E_{red} [a] [V]	HOMO [b] [eV]	LUMO [c] [eV]	E_g [d] [eV]
5a	0.68	-2.39	-5.48	-2.41	3.07
5b	0.13	-2.72	-4.93	-2.08	2.85
6a	0.48	-2.54	-5.28	-2.26	3.02

[a] Estimated from cyclic voltammetric analysis (THF solution). [b] $E(HOMO) = -(E_{ox} + 4.80)$ [eV], where E_{ox} is the onset potential of oxidation, observed in the cyclic voltammetric analyses. [c] $E(LUMO) = -(E_{red} + 4.80)$ [eV], where E_{red} is the onset potential of reduction, observed in the cyclic voltammetric analyses. [d] E_g = E (LUMO) – E (HOMO) [eV].

9. DFT calculation

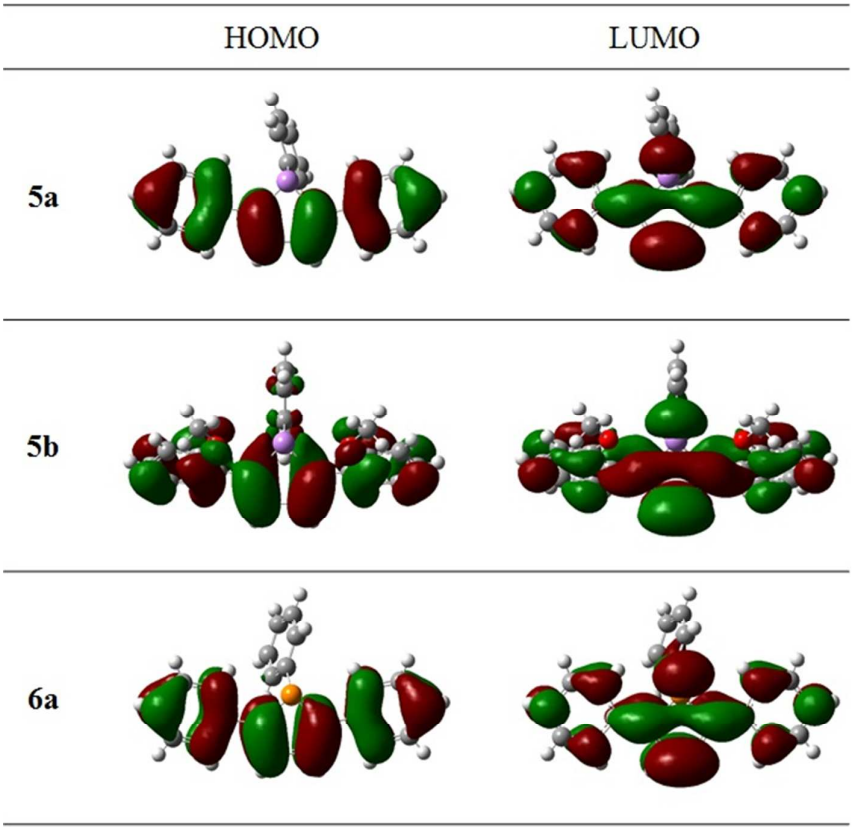

Figure S26. Molecular orbitals for HOMOs and LUMOs of **5a**, **5b** and **6a** calculated at the B3LYP/6-31G+(d,p) level of theory; calculated with the Gaussian 09 suit program.[13]

10. References

1. P. S. Elmes, S. Middleton, B. O. West, *Aust. J. Chem.* **1970**, *23*, 1559.

2. Y. Matsumura, M. Ueda, K. Fukuda, K. Fukui, I. Takase, H. Nishiyama, S. Inagi, I. Tomita, *ACS Macro Lett.* **2015**, *4*, 124.

3. *PROCESS-AUTO, RAXIS data-processing software;* Rigaku Corporation: Tokyo, Japan, 1996.

4. T. Higashi, *FS_ABSCOR, Program for Absorption Correction;* Rigaku Corporation: Tokyo, Japan, 1995.

5. A. C. Larson, *Crystallographic Computing;* F. R. Ahmed, Ed.; Munksgaard: Copenhagen, Denmark, **1970**, 291−294.

6. P. T. Beurskens, G. Admiraal, G. Beurskens, W. P. Bosman, R. de Gelder, R. Israel, J. M. M. Smits, *The DIRDIF-99 Program System;* Technical Report of the Crystallography Laboratory, University of Nijmegen: Nijmegen, The Netherlands, 1999.

7. P. T. Beurskens, G. Admiraal, G. Beurskens, W. P. Bosman, S. Garcia-Granda, R. O. Gould, J. M. M. Smits, C. Smykalla, *PATTY, The DIRDIF Program System;* Technical Report of the Crystallography Laboratory, University of Nijmegen: Nijmegen, The Netherlands, 1992.

8. *CrystalStructure 4.1*: Crystal Structure Analysis Package, Rigaku Corporation (2000-2014). Tokyo 196-8666, Japan.

9. J. R. Carruthers, J. S. Rollett, P. W. Betteridge, D. Kinna, L. Pearce, A. Larsen, E. Gabe, *CRYSTALS Issue 11;* Chemical Crystallography Laboratory: Oxford, U.K., 1999.

10. *SHELXL97*: Sheldrick, G. M (2008). Acta Cryst. A64, 112-122.

11. M. Kumaravel, J. T. Mague, M. S. Balakrishna, *Tetrahedron Lett.* **2014**, *55*, 2957.

12. G. Markl, H. Hauptmann, *Angew. Chem. Int. Ed.* **1972**, *11*, 441.

13. Gaussian 09, Revision C.01, M. J. Frisch, G. W. Trucks, H. B. Schlegel, G. E. Scuseria, M. A. Robb, J. R. Cheeseman, G. Scalmani, V. Barone, B. Mennucci, G. A. Petersson, H. Nakatsuji, M. Caricato, X. Li, H. P. Hratchian, A. F. Izmaylov, J. Bloino, G. Zheng, J. L. Sonnenberg, M. Hada, M. Ehara, K. Toyota, R. Fukuda, J. Hasegawa, M. Ishida, T. Nakajima, Y. Honda, O. Kitao, H. Nakai, T. Vreven, J. A. Montgomery, Jr., J. E. Peralta, F. Ogliaro, M. Bearpark, J. J. Heyd, E. Brothers, K. N. Kudin, V. N. Staroverov, R. Kobayashi, J. Normand, K. Raghavachari, A. Rendell, J. C. Burant, S. S. Iyengar, J. Tomasi, M. Cossi, N. Rega, J. M. Millam, M. Klene, J. E. Knox, J. B. Cross, V. Bakken, C. Adamo, J. Jaramillo, R. Gomperts, R. E. Stratmann, O. Yazyev, A. J. Austin, R. Cammi, C. Pomelli, J. W. Ochterski, R. L. Martin, K.

Morokuma, V. G. Zakrzewski, G. A. Voth, P. Salvador, J. J. Dannenberg, S. Dapprich, A. D. Daniels, Ö. Farkas, J. B. Foresman, J. V. Ortiz, J. Cioslowski, and D. J. Fox, Gaussian, Inc., Wallingford CT, 2009.